J Comput Neurosci (2013) 34:89–101
DOI 10.1007/s10827-012-0408-6

Neural encoding schemes of tactile information in afferent activity of the vibrissal system

Fernando D. Farfán · Ana L. Albarracín · Carmelo J. Felice

Received: 16 November 2011 / Revised: 15 May 2012 / Accepted: 8 June 2012 / Published online: 22 June 2012

Abstract When rats acquire sensory information by actively moving their vibrissae, a neural code is manifested at different levels of the sensory system. Behavioral studies in tactile discrimination agree that rats can distinguish different roughness surfaces by whisking their vibrissae. The present study explores the existence of neural encoding in the afferent activity of one vibrissal nerve. Two neural encoding schemes based on "events" were proposed (cumulative event count and median inter-event time). The events were detected by using an event detection algorithm based on multiscale decomposition of the signal (Continuous Wavelet Transform). The encoding schemes were quantitatively evaluated through the maximum amount of information which was obtained by the Shannon's mutual information formula. Moreover, the effect of difference distances between rat snout and swept surfaces on the information values was also studied. We found that roughness information was encoded by events of 0.8 ms duration in the cumulative event count and event of 1.0 to 1.6 ms duration in the median inter-event count. It was also observed that an extreme decrease of the distance between rat snout and swept surfaces significantly reduces the information values and the capacity to discriminate among the sweep situations.

Keywords Neural coding · Vibrissae (whiskers) · Roughness discrimination · Maximum amount of information · Information theory

Action Editor: Simon R Schultz

Electronic supplementary material The online version of this article (doi:10.1007/s10827-012-0408-6) contains supplementary material, which is available to authorized users.

F. D. Farfán · C. J. Felice
Laboratorio de Medios e Interfases (LAMEIN), Facultad de Ciencias Exactas y Tecnología (FACET), Universidad Nacional de Tucumán (UNT),
Tucumán, Argentina
e-mail: cfelice@herrera.unt.edu.ar

F. D. Farfán (✉) · C. J. Felice
Instituto Superior de Investigaciones Biológicas (INSIBIO), Consejo Nacional de Investigaciones Científicas y Técnicas (CONICET),
Buenos Aires, Argentina
e-mail: ffarfan@herrera.unt.edu.ar

A. L. Albarracín
Laboratorio de Neurociencia, Facultad de Medicina (FM), Universidad Nacional de Tucumán (UNT),
Tucumán, Argentina
e-mail: ana@fm.unt.edu.ar

1 Introduction

Rodents as well as many mammals are characterized by the presence of vibrissae or whiskers located on both sides of the muzzle (Vincent 1912). When rats acquire sensory information by actively moving their vibrissae, a neural code is manifested at different levels of the trigeminal sensory system. During the past 10 years, the neural code at different stages of the whisker sensory pathway has been extensively studied (Arabzadeh et al. 2005, 2006; Mehta et al. 2007; Wolfe et al. 2008; Farfán et al. 2011).

The repetitive application of a stimulus set (static or dynamic) is the experimental paradigm most widely used and accepted for the study of evoked neural responses. These responses are usually grouped into peristimulus time histogram in which the accumulated response to many stimulus presentations is, in effect, averaged (Rogers et al. 2001). The result obtained by this experimental paradigm is called "system response to the stimulus", considering that the system could be a cell or cell population. However, as

others authors have pointed out (Rieke et al. 1997), this is rather unrelated to the problem that the nervous system must solve. The nervous system must often in short order perform accurate and appropriate computations and generate behavioral responses and/or motor commands given just one stimulus presentation, or, more commonly, given a continuously changing stimulus. In this biological scheme, the currency of information content and exchange among and between neurons is the ongoing action potential trains of cells, being them sensory (primary afferent), motor, or any other. The principal challenge for neurophysiologist lies in decoding these spike trains.

Different structures of the neural code have been proposed for texture coding by considering the mechanical characteristics of the vibrissae (resonant frequencies and damping in isolated whiskers) and their location in the whisker pad (Hartmann et al. 2003; Mehta and Kleinfeld 2004; Mitchinson et al. 2004). Arabzadeh et al. (2006) have demonstrated that a texture code would exist in peripheral afferent response of the vibrissal system and that spike rate would be the coding mechanism that underlies textures discrimination in the primary somatosensory cortex.

In this paper, the afferent activity of one vibrissal follicle innervation (average activity) was analyzed, and two biologically plausible neural encoding schemes were proposed. In this sense, we assumed that the roughness information is coded by events of different durations. These events were detected by using an event detection algorithm based on multiscale decomposition of the signal (Continuous Wavelet Transform—CWT). The neural encoding schemes based on events were: the cumulative event count and the inter-event time. Then, the performance of these encoding schemes was evaluated through the maximum amount of information by using the Information Theory (Cover and Thomas 1991; Rieke et al. 1997).

We found that roughness information would be codified by events of 0.6 to 2.0 ms duration, and that two plausible neural encoding schemes would carry that information. On the other hand, it was observed that the discrimination degree among sweep situations would depend on different slip-resistance levels.

2 Materials and methods

2.1 Procedures

Five Wistar adult male rats (300 g–350 g), between 60 and 80 days, were used in our experiments. They were deeply anesthetized with urethane (1.5 g/Kg) and their temperature was maintained at 37° by a servo-controlled heating pad. Surgery consisted of exposing the infraorbital nerve as well as the two branches of the facial nerve (buccal and upper marginal mandibular) on the right side. The motor branches were dissected and transected proximally to avoid possible motor influences on the sensorial pathway. The stimulation electrodes were placed on their distal stumps producing the contraction of the mystacial muscles. The deep vibrissal nerve innervating a vibrissal follicle (DELTA vibrissa) was identified with a high magnification microscope. The dissected nerve was also transected proximally and this action allowed eliminating discharges arriving from higher level of the sensorial pathway. To make sure that the nerve transection did not affect the vibrissal nerve functionality during our recording time, we tested the falling of the nerve afferent activity throughout the time (data not shown). We concluded that the activity starts decreasing 1 h after the nerve section, so we never exceeded this space of time in our experiments. We used a bipolar electrode (insulated silver wire, 0.2 mm diameter) to record the multifiber afferent discharge from deep vibrissal nerve (a branch of the infraorbital nerve), which innervates the follicle of DELTA vibrissa. The recording electrodes as well as the nerves were immersed in a mineral oil bath during all recording.

All these procedures were carried out in accordance with the recommendations of the Guide for the Care and Use of Laboratory Animals (National Research Council, NRC). Depth of anesthesia was ascertained and controlled during the experiment by the lack of either withdrawal reflex to hindlimb pinching or blink reflex to a gentle stimulation of the cornea.

2.2 Recording of vibrissal nerve electrical activity

In this study we have recorded the electrical activity of the DELTA vibrissal nerve (multifiber activity), while the DELTA vibrissa was sweeping surfaces of different roughness. This multifiber activity is the weighted sum of multiple fibers discharges (in short, average activity). The experimental protocol used in this paper has been previously described in detail by Albarracín et al. (2006) and Farfán et al. (2011).

Vibrissa movements were induced by electrical stimulation of facial motor nerve (VII). Square-wave pulses (30 μs, 7 V supramaximal, 10 Hz) simulated vibrissal whisking at its natural frequency. A diagram of the experimental set up is shown in Fig. 1. Nerve activity was recorded and digitized at 20 kHz during a 90 ms window following onset of each cycle of whisker movement (Digidata 1322A, Axon Instruments). Fifty whisker movement cycles were obtained for each surface, and an additional 50 cycles were recorded while whisker moved unobstructed in air as control.

Various studies have shown that rats would implement different behavioral strategies to enhance the acquisition of tactile information (Carvell and Simons 1990; Berg and Kleinfeld 2003; Sachdev et al. 2003). In particular, it was

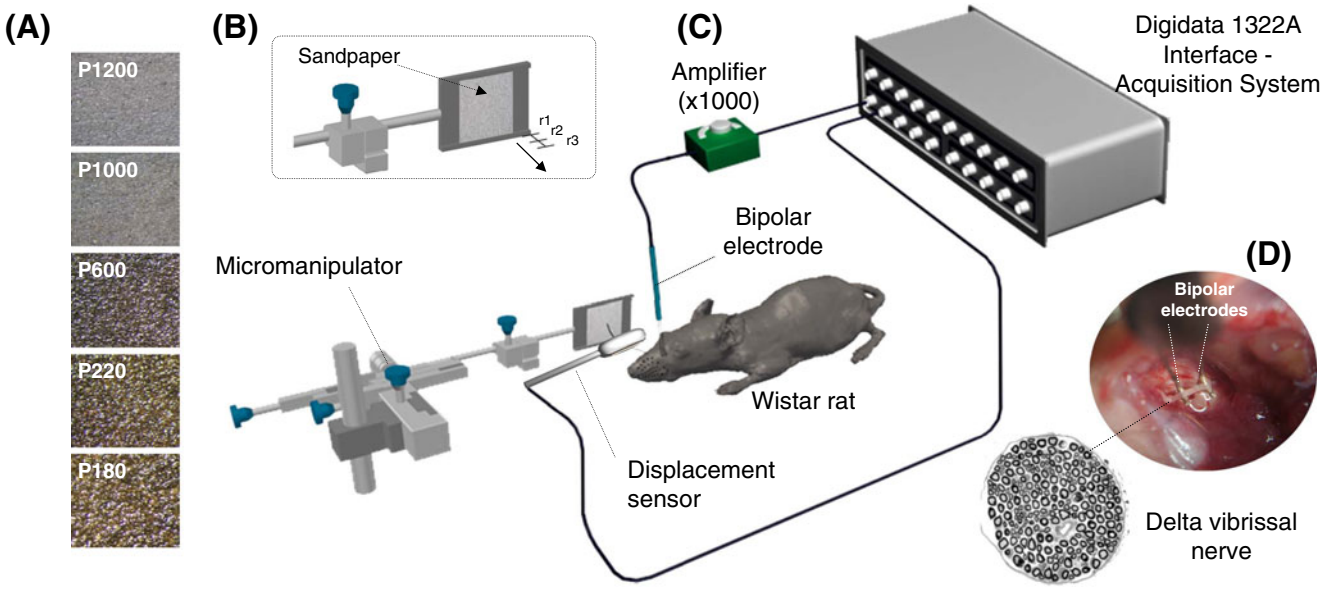

Fig. 1 Experimental procedure. (**a**) Surfaces Pictures. Photographs of the surfaces used in this paper. (**b**) The three slip-resistance levels were obtained by approaching the surfaces. At slip-resistance level 1 (r1), the vibrissa remains in contact with the surface without undergoing deformation. The slip-resistance levels 2 and 3 (r2 and r3) were obtained by using a micromanipulator, and bringing the surfaces closer to the vibrissa by 1 mm each time. (**c**) Preparation used for recording the afferent activity during the sweep on different sandpapers. The micromanipulator is used to control the rough surfaces position and to generate three slip-resistance levels (r1, r2 and r3). Afferent signals are amplified (×1000) and acquired by a Digidata 1322A Interface of Axon Instruments. The acquisition parameters such as sample rate, recording time and data storage are controlled by a personal computer (through Axoscope® software). The whisker movements were measured by using a photoresistive sensor. **(d)** Recording site and placement of recording electrodes. The microphotography below shows the transversal section of the DELTA vibrissal nerve

observed that when a rough surface touch the vibrissal tip (changing the kinematic characteristics of the sweep), the performance for texture discrimination could be modified (Albarracín et al. 2006; Farfán et al. 2011). On the other hand, it is well known that the active whisking on rough surfaces evokes kinematic patterns in vibrissae movements (Wolfe et al. 2008). In this paper, we have varied the distance between rat snout and the swept surface to evaluate a possible behavioral strategy of discrimination. Such behavioral strategy was herein referred to as *slip-resistance levels*, without implying a direct relationship. Importantly, the changes of kinematic patterns evoked by varying the distance between the rat snout and swept surface are unknown.

Thus, three slip-resistance levels were used for each surface. These levels were obtained by mounting the surface at different distances from the whisker base. The minimal level was established by placing the surface at a maximal distance from the whisker base so that the tip just barely contacted the surface (slip-resistance level 1). The following levels were obtained by approaching the surface 1 and 2 mm to the whisker base (slip-resistance levels 2 and 3, respectively).

The DELTA whisker movements were recorded simultaneously with the nerve activity by using a custom-made photoresistive sensor (Fig. 1c). The sensor has a maximal frequency response in the range of 0–100 Hz, enabling direct identification of the protraction and retraction phases of the movement cycle (Dürig et al. 2009). The vibrissal movements were recorded at 20 kHz.

2.3 Rough surfaces

The rough surfaces used in this paper were sandpapers of different grain size: P1200, P1000, P600, P220, and P180 (Fig. 1a). We measured the surfaces roughness by using a Hommel Tester T1000 (Hommel Werke, www.hommel-etamic.de) and we used the Ra parameter (arithmetical deviation of the assessed profile) as a roughness estimation (International Standards BS.1134 and ISO 468). Ra values obtained were: 2.2, 2.9, 5.6, 8.9 and 9.2 μm, respectively.

2.4 Neural codes hypothesis based on events

When the tip or the whisker shaft makes contact with a texture, its movement changes; whisker motion signals report to the brain what the whiskers have contacted (Diamond et al. 2008). In particular, Wolfe et al. (2008) found that when whiskers were moving along the texture, their trajectory was characterized by an irregular, skipping motion: the whisker tip tended to get fixed in place (“stick”), before bending and springing loose (“slip”) only to get stuck again. A slip-stick event was a

jump in speed and acceleration; the two quantities covaried. Thus, a pattern of slip-stick events would be set by surface features like the size of grains and the distance between them (Diamond et al. 2008). Follicular receptors would respond to the most prominent features of the vibrissal movement -the high velocity jumps over texture grains- giving rise to the texture neural code (Arabzadeh et al. 2005; Shoykhet et al. 2000; Ito 1985).

More specifically, follicular receptors transform the mechanical events (slip-tick) to electrical activity (spikes) that would travel through multiple axons (infraorbital nerve) to higher levels. The multifiber activity registered by using bipolar electrodes is inherently averaged into a given time interval. That weighted sum of multiple fibers discharges could be considered as *electrophysiological events* (in short, *events*) in afferent recordings. According to the observations of Diamond et al. (2008) and studies conducted on texture neural coding at peripheral level (Arabzadeh et al. 2006), afferent events could be evoked by the impact of vibrissa with the prominent features of swept surfaces such as grain size and grain spacing. In this paper we have defined the electrophysiological event duration as the time interval in which the activity of multiple axons is temporally and spatially averaged by the recording electrodes (Calvin 1975). We established 0.5 ms as the minimum spike duration, considering the observations made by Albarracín (2008). On the other hand, we stated that the maximum electrophysiological event duration should be the duration of a slip-tick. Wolfe et al. (2008) established that a slip-tick event takes approximately 5 to 10 ms.

Recent investigations have demonstrated that amplitude changes in the average activity of afferent nerve are related to roughness surfaces and slip-resistance levels (Farfán et al. 2011). However, in such studies an encoding scheme at peripheral level has not been shown. In the present study we hypothesize that the amplitude changes in the afferent nerve activity are due to temporal distribution changes of electrophysiological events (TDEE) related to the roughness of the swept surfaces. In short, we propose here neural encoding schemes based on the temporal distribution of events produced by the impact of vibrissae with the mechanical stimuli of rough surfaces.

2.5 Event detection via wavelets

The events in the multifiber recordings were detected by using an event detection algorithm based on multiscale decomposition of the signal (Continuous Wavelet Transform—CWT). The algorithm was proposed by Nenadic and Burdick (2005). The methodology used in the events detection consists of a combination of several techniques stemming from multiresolution wavelet decomposition, statistics, detection theory and estimation theory. Next, we state the five major steps of the algorithm up-front.

1. Multiscale decomposition of the signal using an appropriate wavelet basis.

A wavelet ψ is a function of finite energy and zero average. It is normalized and centered in the neighborhood of the origin. From this function, also called mother wavelet, one can obtain a family of time-scale waveforms by translation and scaling

$$W_{a,b}(t) = \frac{1}{\sqrt{a}}\psi\left(\frac{t-b}{a}\right) \text{ a, b } \in \text{ R} \tag{1}$$

where $a > 0$ represents the scale and b is the translation. The functions $\psi_{a,b}$ are called wavelets and they share the properties of the mother function (Nenadic and Burdick 2005). The wavelet transform of an arbitrary function $x(t)$ is a projection of that function onto the wavelet basis

$$T_x(a,t) = \int_R x(t)\psi_{a,b}(t)\,dt \tag{2}$$

For event detection is important to choose a wavelet that is suitable for the signal of interest. Here, our choice is motivated by the shape of the afferent activity. The mother wavelet used in this paper belongs to the family of biorthogonal wavelets: 'bior1.5' (Daubechies 1992). This wavelet was chosen because its biphasic shape is reminiscent of action potentials recorded with bipolar electrodes (Fig. 1d).

The continuous wavelet transform defined by (2) operates on a continuous set of scales and translations. Hence, the basis functions $\psi_{a,b}$ are not orthogonal and the representation of the signal x by its wavelet coefficients is redundant. Here we choose the set of basis function translations to be finite, where this set is determined by the sampling rate of the signal $f_s(kHz)$ and its duration $T(s)$, i.e., $b \in B$, where $B = \{0,1,\ldots,k,\ldots,N\text{-}1\}$, and $N = Tf_s + 1$ is the number of samples of the discrete signal (time series). Biophysical considerations we used to restrict the relevant scales of the wavelet basis functions. Here, we use a limited set of scales $\boldsymbol{A} = \{a_0, a_1, \ldots, a_j, \ldots a_J\}$, where a_0 and a_J are determined from the signal sampling rate and the minimum and maximum event durations, denoted by W_{min} and W_{max}, respectively. Here we choose the intermediate scales $\{a_1, a_2, \ldots, a_{J-1}\}$ uniformly sampled between the two extrema a_0 and a_J with an arbitrary step. The wavelet decomposition scales were chosen in order to detect events duration from 0.2 to 2.4 msec.

2. To separate the signal and noise at each scale.

By applying the continuous wavelet transform we obtain a multiscale representation of the signal in terms of its wavelet coefficients. If the discrete observations x contain useful signal s and noise w, then the statistical properties of the wavelet coefficients will depend on those of the noise. For purposes of unsupervised signal detection, we must separate these coefficients by estimating the noise level σ

in each coefficient from the sampled data. Then, the noise of each temporal series was eliminated by using simple threshold detection. Donoho proposes to use an adaptive threshold, T, defined using the algorithm introduced in (Donoho 1994). Equations are given in (3) and (4). This algorithm was developed with the assumption that the input to the system consists of spikes added to band-limited white Gaussian noise (Shoham et al. 2003).

$$T_j = \sigma_j \sqrt{2.\log_e(N)} \tag{3}$$

where N is the number of samples of the analyzed time series, σ^2_j is the variance of the noise coefficients $W(j,k)$ at scale a_j and T_j is the threshold of the time series. For a Gaussian random variable, it can be shown that the median of its absolute deviation effectively estimates the standard deviation:

$$\widehat{\sigma}_j = M\left\{\left|X(j,0) - \overline{X}_j\right|, ..., \left|X(j,N-1) - \overline{X}_j\right|\right\}/0.6745 \tag{4}$$

where $\overline{X}_j$ is the simple mean of X_j and $M\{.\}$ denotes the sample median.

3. Detect events at a single scale.

The problem of detecting events in a noisy signal can be seen as a binary hypothesis testing problem, where under the null hypothesis, the signal is not present, and under the alternative, both signal and noise are present. Because of the transient nature of the signal, the alternative hypothesis, if true, will be so only for an interval of time, or equivalently for a subset of the discrete time. Moreover, multiple transients could be present, and these represent the main differences between the problems of classical signal detection and detection of action potentials. The first step of detection problem as a sequential binary hypothesis test at each scale was formulated by Nenadic and Burdick (2005). Thus, the procedures above how to combine the coefficient level decisions and hypothesis testing rule for each wavelet coefficient are available at (Nenadic and Burdick 2005). The hypothesis testing rule for each wavelet coefficient depends upon the acceptable costs of false alarms and omissions and the prior probabilities of the two hypotheses (null and alternative). These factors are related to an acceptance threshold for the alternative hypothesis at each scale. In order to evaluate this threshold the costs of false alarms and omissions should be specified. The algorithm proposed by Nenadic and Burdick (2005), uses a parameter L which is the result of a reparameterization of the relationship between costs of false alarms and omissions (for more details see Nenadic and Burdick 2005). For most practical purposes $-0.2 <= L <= 0.2$. Larger L probably produces omissions, smaller L produce false positives likely.

4. To combine the decisions at different scales.

Because they are highly localized in time, the samples corresponding to neural transients occupy contiguous subsets of the discrete time vector $\boldsymbol{B}$. This property of transients if often referred to as a temporal contiguity. Temporal contiguity translates into the contiguity of coefficients in the wavelet domain (Wang and Willett 2001), i.e., the wavelet coefficients corresponding to the same transient tend to be neighbors in both time and scale. Since the algorithm used here use the continuous wavelet transform with the basis functions of compact support roughly matched to the scale of neural transients, the temporal contiguity in the wavelet domain is inherently preserved. The scale contiguity follows from a broad frequency spread of a time-limited signal, namely if a scale is thought of as an approximation of the frequency, a time-limited transient will be spread across many scales. The presence of noise, however, may obscure the picture at the scales that are not relevant. The scale contiguity can also be viewed in the present context as a cross-correlation (redundancy) of the wavelet coefficients (decisions) at different scales. The problem of redundancy and statistical decision criteria for event detection on multiple scales are formally described in Nenadic and Burdick (2005).

5. To estimate the arrival times of individual events.

In a noise-free environment, the wavelet basis function that provides the maximum correlation with the transient to be detected, corresponds to a wavelet coefficient of maximum magnitude. The time associated with the translation index of the basis function with maximal coefficient can be taken as a good approximation to the occurrence time of the underlying transient. Because we choose the set of translations $\boldsymbol{B}$ with time resolution down to the sampling period, this approximation is essentially as good as the sampling period. Tracking of modulus maxima of the wavelet coefficients across scales has been proposed for the detection of signal singularities (Mallat and Hwang 1992). In a noisy environment, there is naturally a jitter associated with the location of this maximal coefficient. This jitter can be reduced by averaging the locations of the maxima across different scales. This is basically the idea employed in procedures used to estimate the arrival times of individual events.

The MATLAB code of the method and a supporting tutorial are available at: http://robotics.caltech.edu/~zoran/Research/detection.html.

2.6 Neural encoding schemes based on events

Two encoding schemes based on events have been proposed: one based on cumulative event count (hereafter referred to as CEC code) and the other on inter-event time (hereafter referred to as IET code). As described above, each experimental situation consists of 50 sweeps, and hence 50 afferent recordings.

We evaluated the CEC code by measuring the cumulative event count: the buildup of events from stimulus onset until

sometime t_i, at which point the discrimination would be made. The mechanism is illustrated schematically along the time axis in (Fig. 2a). Thus, each experimental situation is represented by 50 values, which are the numbers of events detected in each recording. These values are represented in box plot diagram (Fig. 2a). This procedure is repeated for all experimental situations.

For the IET code, the inter-event time is computed along the whole-whisk (gray zone of Fig. 2b). Then, a median is calculated from the IET values obtained in each sweep. This procedure is repeated for all sweeps and represented in a box plot diagram.

For the CEC code, the discrimination among sweep situations mainly depends on two factors: the window length where the cumulative count is made, and the duration of the events detected. Here, the window length varies from 0 until t_i. For the IET code, the discriminations will only depend on the duration of the detected events. The event durations analyzed for the both schemes were: 0.2, 0.4, 0.6, 0.8, 1.0, 1.2, 1.4, 1.6, 1.8, 2.0, 2.2 and 2.4 ms.

Encoding schemes proposed here are analogous to rate code and temporal code, except that spikes are replaced by events. These schemes will be evaluated by measuring the amount of information that the neuronal response convey about the stimulus. For this purpose it will be used concepts of the information theory (McDonnell et al. 2011).

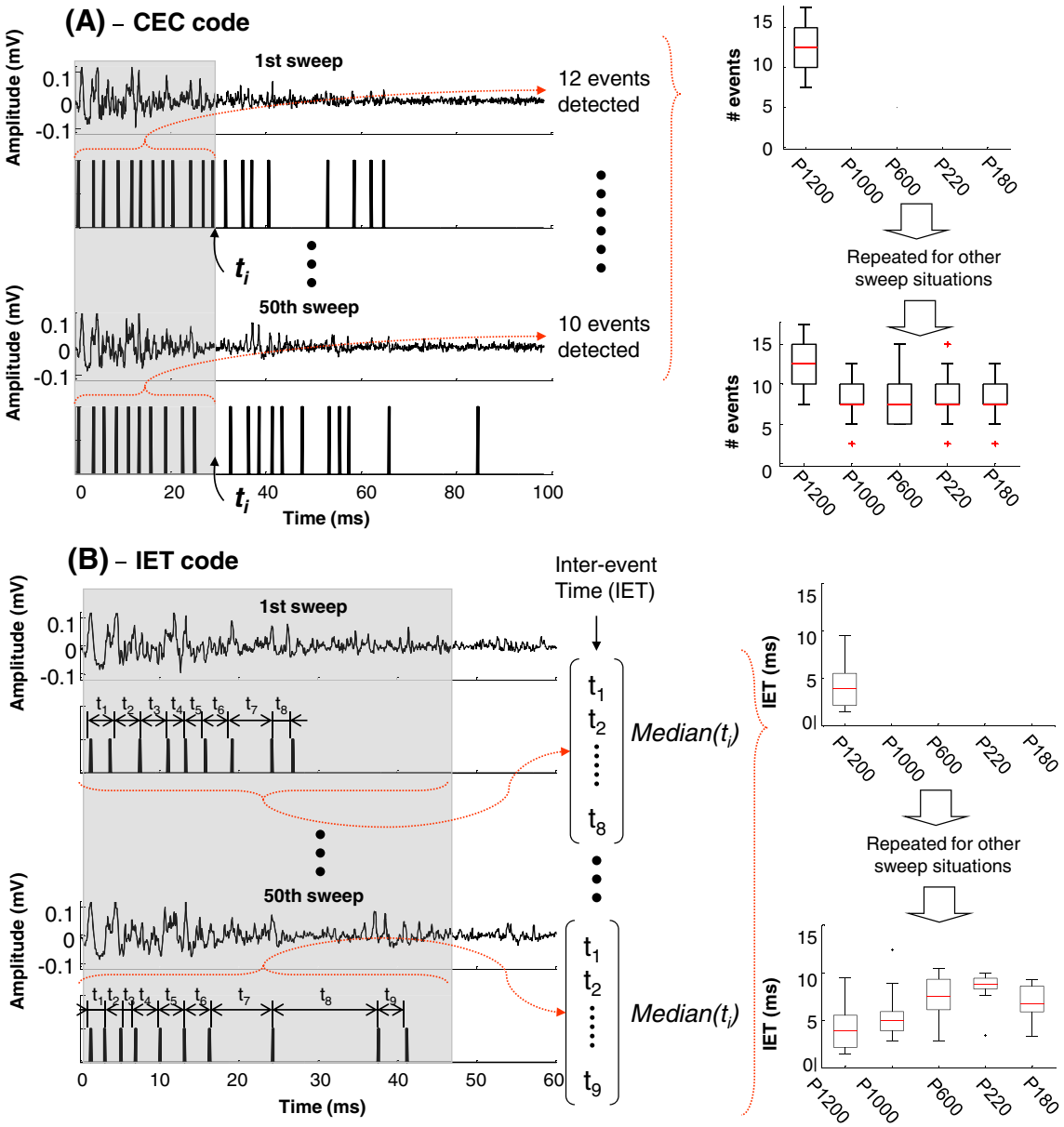

Fig. 2 Neural encoding schemes of tactile information based on events detected in afferent activity. **(a)** CEC code. **(b)** IET code

2.7 Information theory

To determine the amount of information in a biological system it is necessary to have at least a pair of *stimuli/responses* situations. The stimulus may be a time series or simply to belong to a class (for example, Situation 1, situation 2, situation 3,…, situation N). The *response* (*r*) depends on the characteristic of the signal that is being examined. Thus, for example, they can be real values (inter-event time, inter-spikes time, and others) or integer values (number of events/spikes).

The information the neuronal response convey about the stimulus can be quantified by Shannon's mutual information formula (Cover and Thomas 1991), abbreviated hereafter as information:

$$I = \sum P(r).P(s|r)\log_2 \frac{P(s|r)}{P(s)} \tag{5}$$

Where *P(s)* is the probability of presentation of roughness stimulus *s*, *P(s|r)* is the posterior probability of *s* given observation of *r*, and *P(r)* is the probability of *r* unconditional on the stimulus. Information determines the maximum amount of knowledge (the upper bound of information) available to an observer who knows the posterior probabilities *P(s|r)* and uses them to read off the signals available in a single observation of a spike train (Rieke et al. 1997).

In this paper, the stimuli are sweeps situations, P1200, P1000, P600, P220 and P180, and the responses are the inter-event times and the number of events into a time interval. The procedures used to estimate the probabilities of Eq. (5) have been previously described in detail by Farfán et al. (2011). The most important steps are listed below:

1. First, the frequency diagrams (or histograms) are determined. For each experimental situation, the number of occurrences of *r* is obtained. Importantly, the response *r* is a scalar in both coding schemes (CEC and IET codes). For each trial yields an r value (the cumulative event count) in CEC code, while for the IET code, an *r* value is computed from the IET values determined in each trial. Here we used the median of IET values obtained during each trial (the results were not significantly changed when it was used the average of IET values). In this way both encoding schemes will have the same number of responses per experimental situation and may be compared.
2. Determination of the joint probability distribution, *P(s, r)*.
3. Determination of the *P(r)* and *P(s)* probability distributions. The probability of obtaining a response *r*, regardless of whether stimulus *s* did or not occur, is called the marginal probability, and it can be calculated by the sum of joint probabilities for a given response *r*.
4. Determination of conditional probability distribution P (s|r).
5. Determination of the amount of information. After obtaining all probability distributions, it is possible to obtain the mutual information using Eq. (5).

The stimulus-response probabilities in the Eq. (5) are not known a priori and must be estimated empirically from a limited number, N, of experimental trials for each unique stimulus. In our data set, N was 50. Limited sampling of response probabilities can lead to an upward bias in the estimate of information (Optican et al. 1991; Panzeri and Treves 1996; Golomb et al. 1997; Victor 2000; Paninski 2003). We used a number of bias-correction procedures (Panzeri and Treves 1996; Strong et al. 1998; Nemenman et al. 2004). Because they all gave almost identical results, we present only results based on the quadratic extrapolation correction procedure of Strong et al. (1998). This bias correction procedure assumes that the bias can be accurately approximated as second order expansions in $1/N_{tr}^{tot}$ (where N_{tr}^{tot} is the number of trials), that is

$$bias = \frac{a}{N_{tr}^{tot}} + \frac{b}{\left(N_{tr}^{tot}\right)^2} \tag{6}$$

Where *a* and *b* are free parameters that depend on the stimulus-response probabilities, and are estimated by recomputing the information from fractions of the trials as follows. The dataset is first broken into two random partitions and the information quantities are computed for each sub-partition individually: the average of the two partitions provides an estimate corresponding to half of the trials. Similarly, by breaking the data into four random partitions, it is possible to obtain estimates corresponding to a fourth of the trials. Finally, *a* and *b* are extrapolated as parameters of the parabolic function passing through the $N_{tr}^{tot}/2$ and $N_{tr}^{tot}/4$ estimates (Magri et al. 2009).

3 Results

3.1 Recording of afferent activity

The neural activity is conducted from the axons to the electrodes through resistive/capacitive filters (low pass filters), resulting in spikes appearing as weak signals whose shape and amplitude may differ from intracellular spike shapes (Smith and Mtetwa 2007). Further, the activity of distant axons may appear as noise which is highly correlated with the target signal. Therefore, the afferent activity is inevitably corrupted by noise from diverse sources: the recording hardware, the recording environment and the spatially averaged activity of distant axons. All these issues make the problem of the signal analysis a real challenge.

The afferent discharge recorded in our experiments is the average electrical activity of about 200 myelinated axons (Fig. 1d) and not all of those fibers have the same firing patterns. The recording site is shown in (Fig. 1d).

Figure (3a) shows the multifiber recordings belonging to DELTA vibrissa innervation recorded during different sweep situations and for resistance level 1. These recordings show an increase of afferent activity (reflected in its amplitude) in relation to surface roughness and a higher level of activation for slip-resistance level 2.

In all cases the whisker displacements and evoked afferent activity were recorded simultaneously at the same sampling frequency. (Figure 1b) shows the afferent activity evoked by sweeping in air (control) and its corresponding vibrissal displacement. Displacement recordings were used solely to identify the protraction and retraction phases.

3.2 Event detection—coding scheme based on events

The detection algorithm was set up to detect events from 0.2 to 2.4 ms duration. (Figure 3c) shows the afferent activity and events of 0.8 and 1.6 ms duration. As shown, events detected have a significant variability in amplitude. Thus, the events of greater amplitude are the result of spatio-temporal average activity of fibers that are closest to the recording electrodes.

The events durations were established according to results obtained from a preprocessing. Basically, this preprocessing consisted of evaluating events from 0.2 ms to 2.4 ms duration. These results showed that it is not possible to distinguish the experimental situations by using events of <0.6 ms duration. In these cases, the information values were very low (close to zero). Furthermore, few events (or none) of >2 ms duration were detected in the afferent activity. These analyses were performed for the both neural encoding schemes (CEC and IET).

These preliminary results clearly showed that roughness information is relevant for the afferent activity and that it is naturally found in cluster of events with 0.6 to 2.0 ms duration.

3.3 Coding scheme based on cumulative event count

The information values mainly depend on two factors in CEC code: the window length where the cumulative count is made and the duration of events detected. Events of 0.8, 1.0, 1.2 and 1.4 ms duration were the most relevant for CEC code. The slip-resistance protocol as a variable affecting information values was also considered here.

(Figure 4a) (top left) shows the information values obtained for the total stimulus set versus temporal window where the cumulative event count is performed. In this figure we can see

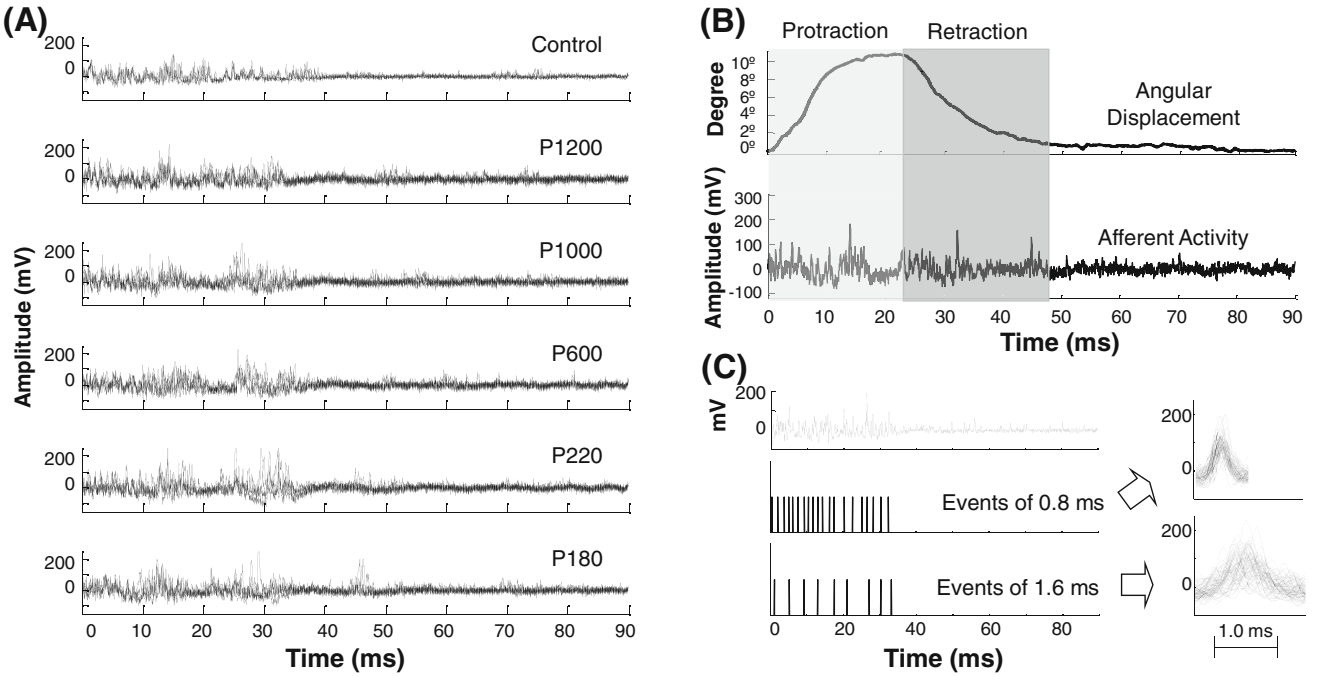

Fig. 3 Afferent discharges and events detected. **(a)** Ten afferent activity recordings obtained during the sweep on: the air (control), sandpaper P1200, sandpaper P1000, sandpaper P600, sandpaper P200 and sandpaper P180. All recordings were registered at slip-resistance level 1. **(b)** Displacement and afferent activity recordings from DELTA vibrissa acquired during a sweep on sandpaper P600. The displacement recordings were acquired by using a custom-made photoresistive sensor. **(c)** Event detection from afferent activity recording during a sweep on sandpaper P1000 (above). Events temporal location of 0.8 and 1.6 ms duration are shown in figures lower down. The detected events are shown on the right side

that the most important events for the CEC code have durations of 0.8 and 1.0 ms (i.e. information values obtained with these events durations are significant). On the other hand, we observe that higher information values (I>1 bit) were obtained between 7 and 33 ms, period of time that mainly corresponds to the protraction phase.

By increasing the slip-resistance level, the information was greater than 1 bit in the range of 28 ms to 50 ms, which mainly covers the retraction phase (Fig. 4b). It can be also note that information provided by events of 1.0 ms duration decreased considerably. All information values decreased significantly at slip-resistance 3 (Fig. 4c).

The information obtained from stimulus pairs was also analyzed. Thus, events of 0.8 ms duration mainly contribute to the information obtained from the pair P1200–P1000. For slip-resistance level 1, the most significant information values are given for the retraction phase (Fig. 4a, top right), but for slip-resistance level 2 the maximum information values are reduced to the range between 23 and 35 ms (Fig. 4b, middle right). Like values obtained with total stimulus set, the information values obtained from the pair P1200–P1000 decrease considerably at slip-resistance level 3 (Fig. 4b, bottom right). Results for all possible pairwise comparisons are shown in Additional files 1, 2 and 3 (slip-resistances 1, 2 and 3, respectively).

Figure (5) shows the matrices of all pairwise information values for the different slip-resistance levels. These results illustrate pairwise stimulus discriminability by using CEC code at peripheral level (events of 0.8 ms duration). Rows and columns are labeled by a stimulus, and gray scale entries give the information available between the two corresponding stimuli. At slip-resistance level 1, the stimulus pair with the highest degree of discriminability (more information) is P220–P1200 (0.4 bits). The information values were approximately 0.4 bits for comparisons between stimulus pairs P220–P1000 and P220–P600. The increase of the slip-resistance from level 1 to level 2, improved the degree of discriminability for the stimulus pairs P1200–P1000, P1200–P220, P600–P180 and P600–P180 (Fig. 5). Finally, at slip-resistance level 3, the information values decreased significantly in most cases (except P600–P220).

3.4 Coding scheme based on IET

The IET were obtained from events of 0.2 to 2.4 ms duration. The analysis showed that events shorter than 0.6 ms duration and longer than 2.0 ms duration do not provide relevant information about stimuli. Then, the IET code was evaluated considering the total stimulus set and the pair wise stimulus at different slip-resistance levels.

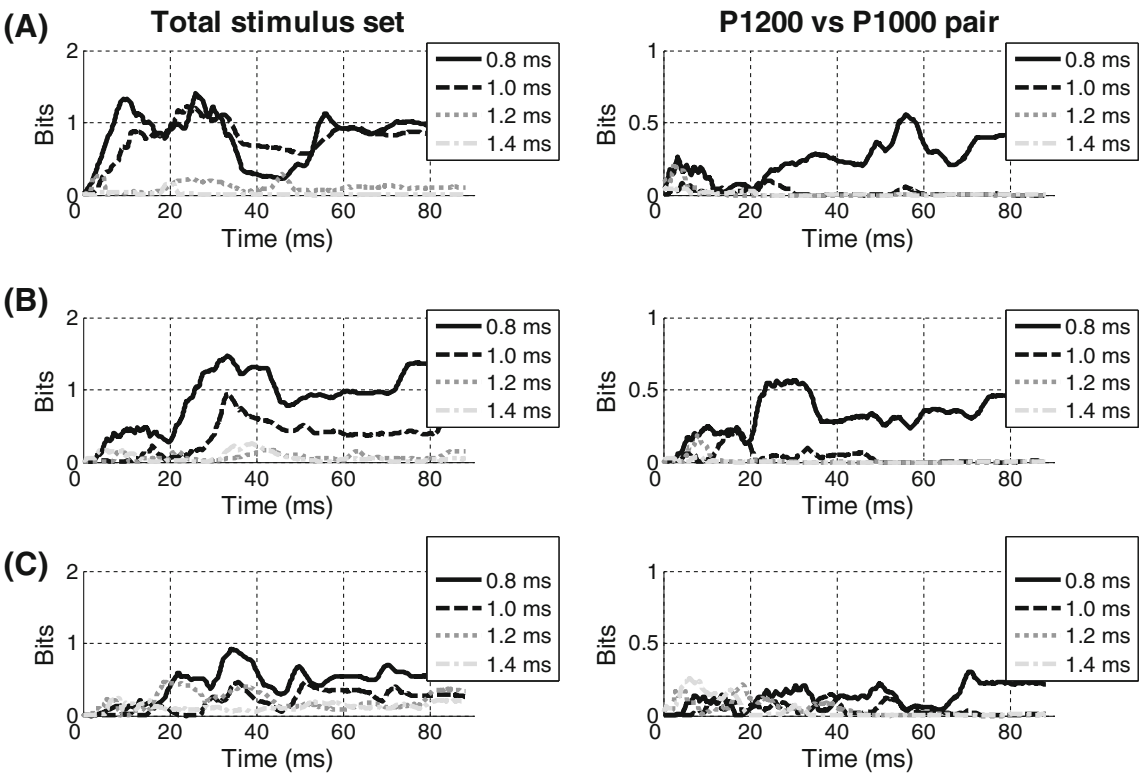

Fig. 4 Information values versus window length where the cumulative event count is done. **(a)** The information values were obtained considering the total stimulus set (*left*) and the stimulus pair P1200–P1000 (*right*). The events depicted in these figures were of 0.8, 1.0, 1.2 and 1.4 ms durations. These results were obtained at slip-resistance level 1. **(b)** Idem to A, but using the slip-resistance level 2. **(c)** Idem to A, but using the slip-resistance level 3

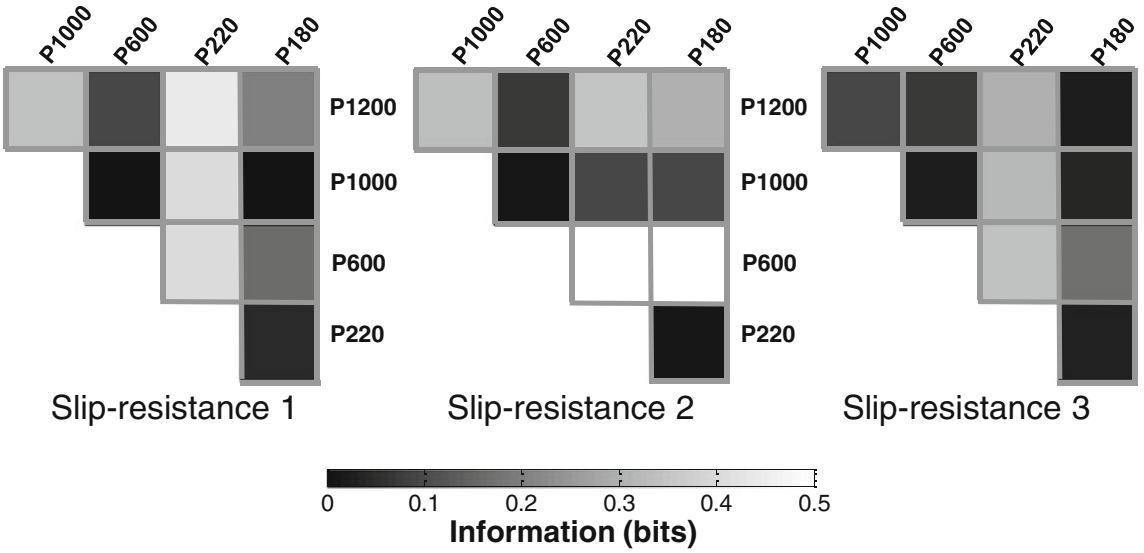

Fig. 5 Matrix of all pairwise information values for slip-resistance level 1 (*left*), slip-resistance level 2 (*middle*) and slip-resistance level 3 (*right*). Event duration considered for these calculations were of 0.8 ms

The information values for the total stimulus set were higher for events longer than 1 ms duration. (Figure 6) shows that the information values vary according to the event duration and the different slip-resistance levels. In particular, the information values decrease with the increase of slip-resistance level for events of 1.0, 1.4 and 2.0 ms duration. However, increases of information values were observed when slip-resistance increased from level 1 to 2 for the remaining event durations. These increases of information values are related to a better discrimination among sweep situations. Then, information decreased when the slip-resistance increased from 2 to 3 for all cases. This particularity indicates that the stimuli discriminability has decreased.

The P1200 versus P1000 could be slightly discriminated through the IET code by considering events between 1.0 ms and 1.8 ms duration (Fig. 7, top left) at slip-resistance level 1. It was possible to note that the discriminability between these experimental situations increases with slip-resistance levels.

The discrimination of P1200 versus P180 was maximum for events of 1.0 ms at slip-resistance level 1, and for events of 1.2 ms at slip-resistance level 2. Likewise, it was possible to note that at slip-resistance level 3, the information increased for events of 1.4 ms duration (Fig. 7, top right). P600 could be optimally discriminated from P180 with events of 1.0, 1.2 and 1.4 ms duration at slip-resistance level 2 (Fig. 7, bottom left), while P220 versus P180 could be discriminated with events of 1.2 and 1.4 ms duration at slip-resistance level 1 (Fig. 7, bottom right).

Although we only show four pairwise stimuli (Fig. 7), all possible combinations were analyzed. Additional file 4 shows the information values belonging to all pairwise stimuli.

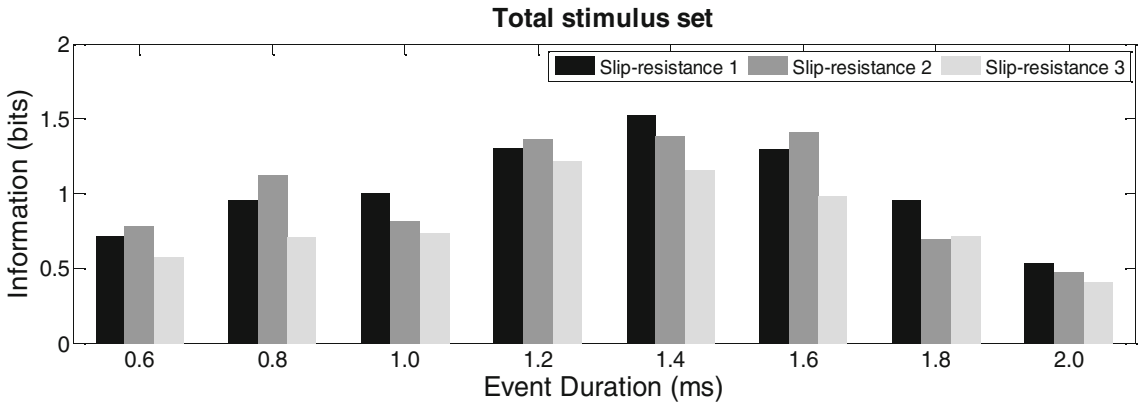

Fig. 6 Information values obtained for the total stimulus set at different slip-resistance levels. Event duration considered for these calculations were of 0.6 to 2.0 ms. The remaining event durations showed no significant information values

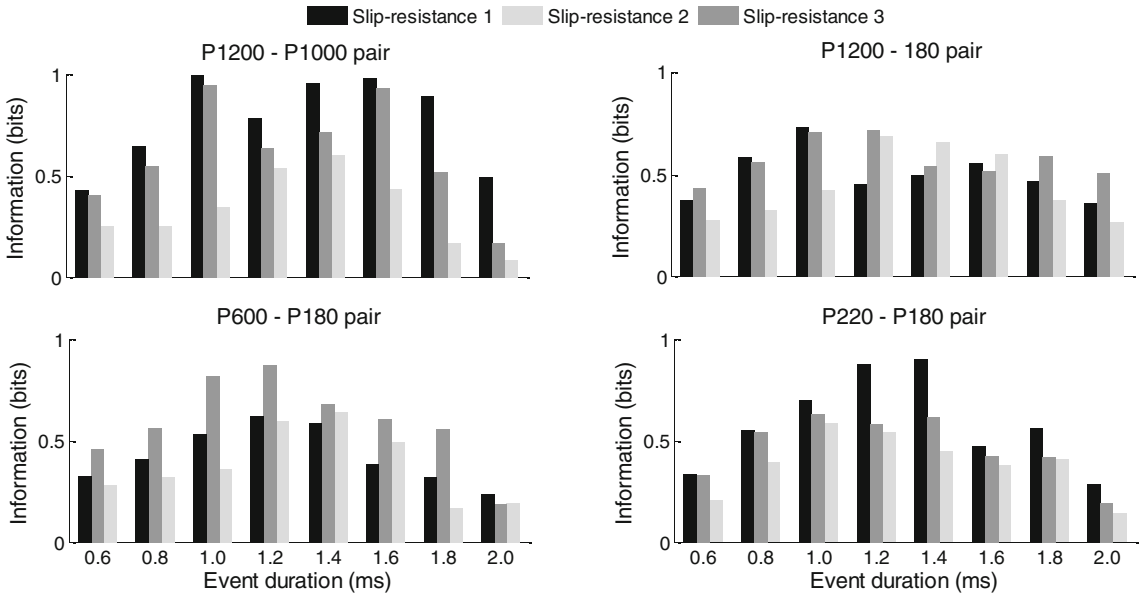

Fig. 7 Information values obtained for some stimulus pairwise at different slip-resistance levels. Event duration considered for these calculations were of 0.6 to 2.0 ms. The remaining event durations showed no significant information values

4 Discussion

In general, inferences about systems behaviour (neural encoding) from specific observations (such as single-unit recordings) are very difficult. In particular, the texture encoding in the vibrissal system comes being studied from the neural activity of one or a few neurons of trigeminal ganglion and/or cortex (Arabzadeh et al. 2005, 2006). Ideally, whether information from each constituent element of the system is obtained, then the system could be fully described. However, this would be practically impossible due to the complexity of necessary instruments. Here, the afferent activity related to texture information was obtained from entire follicular innervation of a DELTA vibrissa. This approach was also implemented at Albarracín et al. 2006, and Farfán et al. 2011.

Wolfe et al. (2008), demonstrated the existence of kinematic patterns (slip-stick events) in the rat vibrissae during the active touch on rough surfaces. Then, Diamond et al. (2008), carried out a review about the way those kinematic patterns would be related to both electrophysiological activity at peripheral and central levels. On the other hand, our previous investigations have shown that roughness information can be analyzed and characterized through afferent activity of a single vibrissa innervation. Based on these studies, we have hypothesized that the tactile sensory information could be carried by spikes trains, which are seen as events in afferent activity recordings when a bipolar electrode is placed on the vibrissal nerve.

In the current study, the afferent nerve activity—from 200 myelinated axons—was the result of phase summation and cancellation of single fiber potentials. Thus, the afferent activity amplitude depends on axons diameter and the distribution of the axons diameter in relation to the recording electrode. In this sense, the complexity of multifiber recordings (activity of about 200 myelinated axons) is an important factor, which presents advantages and disadvantages when a system behavior is studied.

Albarracín et al. (2006) have shown that the changes of afferent signal amplitude would be related to different levels of mechanoreceptors activation, while Farfán et al. (2011) have demonstrated that these amplitude changes could be roughness surfaces dependent. Here, a more detailed analysis was performed over the afferent signal. The event detection algorithm was able to detect events from 0.2 to 2.4 ms duration in the afferent signal, and it seems that the roughness information was naturally found in cluster of events of 0.6 to 2.0 ms duration.

In particular, we found that roughness information was encoded by events of 0.8 ms duration in the CEC code and event of 1.0 to 1.6 ms duration in the IET code. The best discriminability among stimuli was found for the slip-resistance level 2. This result agrees with those obtained by Farfán et al. (2011). It was also observed that an excessive decrease of slip-resistance level significantly reduces the degree of discriminability among the sweep situations.

In previous studies we presented evidence that afferent discharge amplitude changed due to roughness surfaces and slip-resistance levels. This allows to speculate that roughness information is slip-resistance dependent at peripheral level, although the amplitude of the afferent activity is not a biologically plausible neural coding scheme of texture. Here, we have shown that the amplitude changes could be due to events

of different durations that would carry roughness information through two biologically plausible neural code schemes.

4.1 Neural coding and surfaces morphology

Authors such as Arabzadeh et al. (2006), Petersen et al. (2009), Panzeri and Diamond (2010) and others (Diamond et al 2008; Panzeri et al. 2001; Petersen et al 2001; Petersen et al. 2002), have used the information theory to investigate which features of ensemble neuronal activity report information about whisker stimuli. In all of them, the information was calculated based on the equiprobability of presentation of roughness stimulus *P(s)*, Eq. (5). However, roughness measurements obtained here show that *P(s)* would not have equally likely. Thus, less rough surfaces P1200 and P1000 have a difference of 0.7 μm (Ra= 2.2 and 2.9 μm respectively), while P1000 and P600 have a difference of 2.7 μm (Ra=2.9 and 5.6 μm respectively). According to these measurements, it would be more difficult to distinguish between P1200 and P1000 pair than between P1000 and P600 pair. The roughness difference between P220 and P180 is only 0.3 μm (8.9–9.2 μm respectively). Then, P220–P180 pair would be more difficult to discriminate than P1200–P1000 pair. This inference is supported by information values obtained in the CEC and IET codes.

The sweep surface morphology is a very important factor, since of this would depend on the characteristics of kinematic patterns evoked during the active sweep (Wolfe et al. 2008). However, surface texture is not a measurable quantity; it is not possible to assign a unique "texture" value to every different surface. Despite this, it is possible to measure some of the intrinsic characteristics, or parameters of surface texture. In this way, it would be possible to carry out better estimates of *P(s)* by measuring some intrinsic characteristics of surfaces morphology. Here, *P(s)* were considered equally likely in order to compare our results with those obtained by other authors.

A quantitative knowledge of surface morphology could improve the understanding of the tactile information encoding. This is a crucial point to further understand the tactile information processing. Based on the existence of electrophysiological events in afferent signal, and its possible coding schemes, it is possible to speculate that CEC code could provides information about the number of kinematic events evoked in the whiskers by surface irregularities, while the IET code could provides information about the spatial distribution of these kinematic events. These speculations are supported by the current knowledge of sensory processing of tactile information in vibrissal system.

4.2 Considerations of facial nerve stimulation and whisker movement

Most of studies in active whisking deliver a train of pulses throughout the protraction (Szwed et al. 2003; Arabzadeh et al. 2005); while this generates more realistic motions, it also introduces concerns about stimulus artifacts. In this paper, the motions are shorter than typical (~25 ms protraction in (Fig. 3b) compared to ~60 msec in awake animals and other electrical whisking studies). This is because only a square-wave pulse (30 μs, 7 V supramaximal, 10 Hz) is applied to the facial nerve to produce a whisker movement. This stimulation evokes whisking movements that differ from those produced during natural whisking. Despite this, our experimental protocol allows to record and to analyze the afferent activity without stimulus artifacts. In our experimental set-up, the facial nerve stimulation with train pulses would contaminate the afferent activity recordings with stimulus artifacts, and therefore, the processing techniques proposed here could not be used.

Finally, although the artificial whisking movements are different to the natural whisking, the slip-tick events evoked by vibrissa sweeping on roughness surfaces (Wolfe et al. 2008) could be similar to those produced during natural sweeping.

5 Conclusions

In this paper we have demonstrated the existence of two biologically plausible neural encoding schemes of tactile information based on electrophysiological events, and we also showed that the performance of such neural encoding schemes depend on the distance between rat snout and swept surfaces. This last observation suggests that slip-resistance would be a possible behavioral strategy for rough surfaces discrimination.

Acknowledgements This work has been supported by grants from Agencia Nacional de Promoción Científica y Tecnológica (ANPCYT); Consejo Nacional de Investigaciones Científicas y Técnicas (CONICET), and Consejo de Investigaciones de la Universidad Nacional de Tucumán (CIUNT), as well as with Institutional funds from Instituto Superior de Investigaciones Biológicas (INSIBIO).

References

Albarracín, A. L., Farfán, F. D., Felice, C. J., & Décima, E. E. (2006). Texture discrimination and multi-unit recording in the rat vibrissal nerve. *BMC Neuroscience, 7*, 42.

Albarracín, A. L. (2008). Estudio fisiológico y anatómico del control motor de las vibrisas de la rata. PhD Thesis.

Arabzadeh, E., Panzeri, S., & Diamond, M. E. (2006). Deciphering the spike train of a sensory neuron: counts and temporal patterns in the rat whisker pathway. *The Journal of Neuroscience, 26*(36), 9216–9226.

Arabzadeh, E., Zorzin, E., & Diamond, M. E. (2005). Neuronal encoding of texture in the whisker sensory pathway. *PLoS Biology, 3*, e17.

Berg, R. W., & Kleinfeld, D. (2003). Rhythmic whisking by rat: retraction as well protraction of the vibrissae is under active muscular control. *Journal of Neurophysiology, 89*, 104–117.

Calvin, W. H. (1975). Generation of spike trains in CNS neurons. *Brain Research, 84*, 1–22.

Carvell, G. E., & Simons, D. J. (1990). Biometric analyses of vibrissal tactile discrimination in the rat. *Journal of Neuroscience, 10*, 2638–2648.

Cover, T. M., & Thomas, J. A. (1991). *Elements of information theory*. New York: Wiley.

Daubechies, I. (1992). *Ten lectures on wavelets*. Philadelphia: SIAM.

Diamond, M. E., von Heimendahl, M., & Arabzadeh, E. (2008). Whisker-mediated texture discrimination. *PLoS Biol, 6*(8), e220.

Donoho, D. L. (1994). Nonlinear wavelet methods for recovery of signals, densities, and spectra from indirect and noisy data. Proc Sympos Appl Math. 173–205.

Dürig, F., Albarracín, A. L., Farfán, F. D., & Felice, C. J. (2009). Design and construction of a photoresistive sensor for monitoring the rat vibrissal displacement. *Journal of Neuroscience Methods, 80*(1), 71–76.

Farfán, F. D., Albarracín, A. L., & Felice, C. J. (2011). Electrophysiological characterization of texture information slip-resistance dependent in the rat vibrissal nerve. *BMC Neuroscience, 12*, 32.

Golomb, D., Hertz, J., Panzeri, S., Treves, A., & Richmond, B. (1997). How well can we estimate the information carried in neuronal responses from limited samples? *Neural Computation, 9*, 649–665.

Hartmann, M. J., Johnson, N. J., Towal, R. B., & Assad, C. (2003). Mechanical characteristics of rat vibrissae: resonant frequencies and damping in isolated whiskers and in the awake behaving animal. *J Neuroscience, 23*(16), 6510–6519.

Ito, M. (1985). Processing of vibrissa sensory information within the rat neocortex. *Journal of Neurophysiology, 54*, 479–490.

Magri, C., Whittingstall, K., Singh, V., Logothetis, N. K., & Panzeri, S. (2009). A toolbox for the fast information analysis of multiple-site LFP, EEG and spike train recordings. *BMC Neuroscience, 10*(1), 81.

Mallat, S., & Hwang, W. L. (1992). Singularity detection and processing with wavelets. *IEEE Trans Inform Theory, 38*(2), 617–643.

McDonnell, M. D., Ikeda, S., & Manton, J. H. (2011). An introductory review of information theory in the context of computational neuroscience. *Biological Cybernetics, 105*, 55–70.

Mehta, S. B., & Kleinfeld, D. (2004). Frisking the whiskers: patterned sensory input in the rat vibrissae system. *Neuron, 41*, 181–184.

Mehta, S. B., Whitmer, D., Figueroa, R., Williams, B. A., & Kleinfeld, D. (2007). Active spatial perception in the vibrissa scanning sensorimotor system. *PLoS Biology, 5*(2), e15. doi:10.1371/journal.pbio.0050015.

Mitchinson, B., Gurney, K. N., Redgrave, P., Melhuish, C., Pipe, A. G., Pearson, M., Gilhespy, I., & Prescott, T. J. (2004). Empirically inspired simulated electromechanical model of the rat mystacial follicle-sinus complex. *Proceedings of the Royal Society of London, 271*, 2509–2516.

Nemenman, I., Bialek, W., & van Steveninck, R. (2004). Entropy and information in neural spike trains: progree on the sampling problem. *Physical Review E, 69*, 056111.

Nenadic, Z., & Burdick, J. W. (2005). Spike detection the continuous wavelet transform. *IEEE Transactions on Biomedical Engineering, 52*(1), 74–87.

Optican, L. M., Gawne, T. J., Richmond, B. J., & Joseph, P. J. (1991). Unbiased measures of transmitted information and channel capacity from multivariate neuronal data. *Biological Cybernetics, 65*, 305–310.

Paninski, L. (2003). Convergence properties of three spike-triggered analysis techniques. *Network, 14*, 437–464.

Panzeri, S., & Diamond, M. E. (2010). Information carried by population spike times in the whisker sensory cortex can be decoded without knowledge of stimulus time. *Frontiers in Synaptic Neuroscience*, *2*(17).

Panzeri, S., Petersen, R. S., Schultz, S., Lebedev, M., & Diamond, M. E. (2001). The role of spike timing in the coding of stimulus location in rat somatosensory cortex. *Neuron, 29*, 769–777.

Panzeri, S., & Treves, A. (1996). Analytical estimates of limited sampling biases in different information measures. *Network, 7*, 87–107.

Petersen, R. S., Panzeri, S., & Diamond, M. E. (2001). Population coding of stimulus location in rat somatosensory cortex. *Neuron, 32*, 503–514.

Petersen, R. S., Panzeri, S., & Diamond, M. E. (2002). Population coding in somatosensory cortex. *Current Opinion in Neurobiology, 12*, 441–447.

Petersen, R. S., Panzeri, S., & Maravall, M. (2009). Neural coding and contextual influences in the whisker system. *Biological Cybernetics, 100*(6), 427–446.

Rieke, F., Warland, D., Ruyter, D., van Steveninck, R., & Bialek, W. (1997). *Spikes: exploring the neural code*. Cambridge: MIT Press.

Rogers, R. F., Runyan, J. D., Vaidyanathan, G., & Schwaber, J. S. (2001). Information theoretic analysis of pulmonary stretch receptor spike trains. *Journal of Neurophysiology, 85*, 448–461.

Sachdev, R. N. S., Berg, R. W., Champney, G., Kleinfeld, D., & Ebner, F. F. (2003). Unilateral vibrissa contact: changes in amplitude but not timing of rhythmic whisking. *Somatosensory & Motor Research, 20*, 163–169.

Shoykhet, M., Doherty, D., & Simons, D. (2000). Coding of deflection velocity and amplitude by whisker primary afferent neurons: implications for higher level processing. *Somatosens Motor Res, 17*, 171–180.

Shoham, S., Fellows, M. R., & Normann, R. A. (2003). Robust, automatic spike sorting using mixtures of multivariate t-distributions. *Journal of Neuroscience Methods, 127*, 111–122.

Smith, L. S., & Mtetwa, N. (2007). A tool for synthesizing spike trains with realistic interference. *Journal of Neuroscience Methods, 159* (1), 170–180.

Strong, S. P., Koberle, R., van Steveninck, R., & Bialek, W. (1998). Entropy and information in neural spike trains. *Physical Review Letters, 80*, 197–200.

Szwed, M., Bagdasarian, K., & Ahissar, E. (2003). Encoding of vibrissal active touch. *Neuron, 40*(3), 621–630.

Victor, J. D. (2000). Asymptotic bias in information estimates and the exponential (Bell) polynomials. *Neural Computation, 12*, 2797–2804.

Vincent, S. B. (1912). The function of the vibrissae in the behavior of the white rat. *Behav Monog, 1*, 1–181.

Wang, Z., & Willett, P. K. (2001). All-purpose plug-in power-law detectors for transients signals. *IEEE Trans Signal Processing, 49*(11), 2454–2466.

Wolfe, J., Hill, D. N., Pahlavan, S., Drew, P. J., Kleinfeld, D., et al. (2008). Texture coding in the rat whisker system: slip-stick versus differential resonance. *PLoS Biology, 6*(8), e215.